nature biotechnology

Optimization of humanized IgGs in glycoengineered *Pichia pastoris*

Huijuan Li[1], Natarajan Sethuraman[1], Terrance A Stadheim[1], Dongxing Zha[1], Bianka Prinz[1], Nicole Ballew[1], Piotr Bobrowicz[1], Byung-Kwon Choi[1], W James Cook[1], Michael Cukan[1], Nga Rewa Houston-Cummings[1], Robert Davidson[1], Bing Gong[1], Stephen R Hamilton[1], Jack P Hoopes[2], Youwei Jiang[1], Nam Kim[1], Renee Mansfield[1], Juergen H Nett[1], Sandra Rios[1], Rendall Strawbridge[2], Stefan Wildt[1] & Tillman U Gerngross[3]

As the fastest growing class of therapeutic proteins, monoclonal antibodies (mAbs) represent a major potential drug class[1]. Human antibodies are glycosylated in their native state and all clinically approved mAbs are produced by mammalian cell lines, which secrete mAbs with glycosylation structures that are similar, but not identical, to their human counterparts. Glycosylation of mAbs influences their interaction with immune effector cells that kill antibody-targeted cells[2–6]. Here we demonstrate that human antibodies with specific human N-glycan structures can be produced in glycoengineered lines of the yeast *Pichia pastoris* and that antibody-mediated effector functions can be optimized by generating specific glycoforms. Glycoengineered *P. pastoris* provides a general platform for producing recombinant antibodies with human N-glycosylation.

Monoclonal antibodies often achieve their therapeutic benefit through two binding events. First, the variable domain of the antibody binds a specific protein on a target cell (for example, CD20 on the surface of cancer cells). This is followed by recruitment of effector cells such as natural killer (NK) cells that bind to the constant region (Fc) of the antibody and destroy cells to which the antibody has bound. This process, known as antibody-dependent cell cytotoxicity (ADCC), depends on a specific N-glycosylation event at Asn 297 in the Fc domain of the heavy chain of IgG1s[2]. Antibodies that lack this N-glycosylation structure still bind antigen but cannot mediate ADCC, apparently as a result of reduced affinity of the Fc domain of the antibody for the Fc receptor FcγRIIIa on the surface of NK cells. (NK cells are positive for CD56, CD16 (FcγRIIIa); and do not express FcγRI, FcγRIIa, FcγRIIb or FcγRIIIb). Not only is ADCC dependent on glycosylation of the Fc domain, but the degree of cell-mediated killing is sensitive to the composition of the glycans in the Fc region of the antibody[2]. This finding prompted studies to determine the impact of glycosylation on cell-mediated killing. These involved IgGs produced by different mammalian cell lines so that they possessed identical amino acid sequences but varying glycan compositions[3–6]. As each of these cell lines produce a number of different glycoforms, it was difficult to deconvolute the complexity of this information and relate specific binding affinities to specific glycan structures and their corresponding ADCC activities. Notwithstanding these complications, general structural characteristics such as the lack of fucose or the presence of bisecting N-acetyl glucosamine have been positively correlated with the potency of ADCC[2,4–6].

The elucidation of glycosylation-dependent ADCC is generally complicated by the fact that although this event requires the recruitment of NK cells mediated by the interaction of Fc with FcγRIIIa, interaction of Fc may also occur with several other Fcγ receptors that are present on a number of different cell types. This may interfere with NK-mediated ADCC. Some of these Fcγ receptor-binding events have been analyzed in more detail, and involve specific stimulatory receptors (for example, FcγRIIIa)[5] as well as inhibitory receptors (for example, FcγRIIb that is not expressed in NK cells)[7]. This is clinically important, as there are polymorphic variants of FcγRIIIa in humans, a particular subset of which contains either a valine or phenylalanine at amino acid 158. The former variant (V158) has a significantly higher binding affinity for Fc than the latter (F158)[5]. A more recent clinical study attempted to correlate survival of non-Hodgkins lymphoma patients treated with rituximab (Rituxan, an anti-CD20 antibody) with FcγRIIIa receptor polymorphisms in these patients[8]. The authors demonstrated by multivariant analysis that the V158 variant was the single parameter associated with improved clinical and molecular responses to rituximab, suggesting both that Fc binding affinity to FcγRIIIa is clinically relevant, and that antibodies with higher potency could be developed by modulating the Fc/FcγRIIIa interaction. In a murine melanoma model, the inhibition of ADCC associated with binding of Fc to FcγRIIb suggests that optimal cell-mediated killing may be achieved by increasing binding to FcγRIIIa while reducing binding to FcγRIIb[7]. Here we show through antibody glycoengineering that particular glycosylation-dependent Fcγ receptor-binding affinities can be optimized.

[1]GlycoFi Inc. 21 Lafayette Street, Lebanon, New Hampshire, 03766, USA. [2]Department of Surgery, Dartmouth-Hitchcock Medical Center, Lebanon, New Hampshire 03766, USA. [3]Thayer School of Engineering, Department of Biological Sciences and the Department of Chemistry, Dartmouth College, Hanover, New Hampshire 03755, USA. Correspondence should be addressed to T.U.G. (tillman.gerngross@dartmouth.edu).

Received 17 August 2005; accepted 18 November 2005; published online 22 January 2006; doi:10.1038/nbt1178

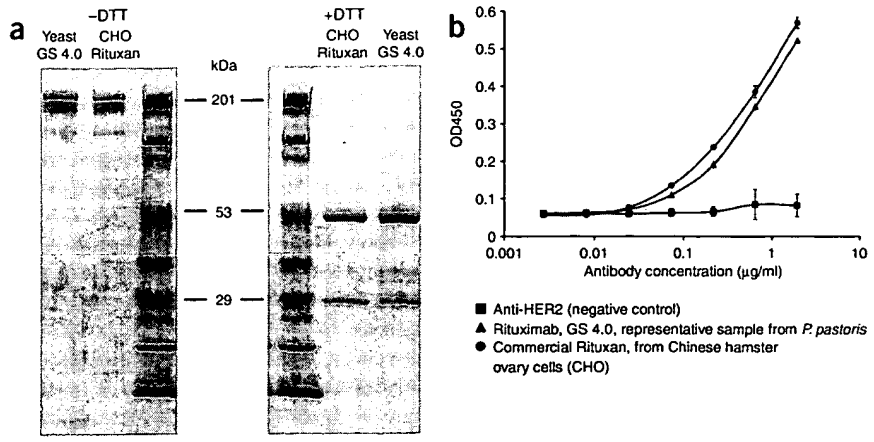

Figure 1 Characterization of yeast-derived antibody. SDS-PAGE of commercial rituximab, that is, Rituxan (product derived from CHO cells) and rituximab derived from glycoengineered yeast (GS4.0). (**a**) Nonreducing gel (left panel) and reducing gel (right panel). (**b**) Binding of rituximab variants to CD20 antigen on WIL2-S cells.

Previously, we engineered several yeast cell lines to perform specific human N-glycosylation reactions with high fidelity[9–11]. Whereas mammalian cell lines produce a mixture of glycoforms and typically do not permit the control of glycosylation, glycoengineered yeast cell lines can produce more uniform glycoproteins and allow unprecedented control over glycosylation[12]. In this study we use several glycoengineered lines of *P. pastoris* to produce a library of glycoforms of the anti-CD20 antibody rituximab and compare their receptor binding properties to the mammalian cell–derived commercial counterpart Rituxan. It is noteworthy that the polypeptide backbone of these antibody variants are identical and that only the glycosylation structures differ. Differences in function are thus a property mediated by the glycan composition at Asn 297 and not the amino acid sequence. However, other common modifications found on mammalian cell culture–derived antibodies such as deamination, methionine oxidation, proteolytic cleavage and C-terminal lysine cleavage may or may not be present on the yeast-derived antibody variants, and their absence may contribute to some of the improved function.

Heavy and light chains of rituximab were expressed in several different glycoengineered *P. pastoris* lines, as well as in a wild-type strain[9–11]. The antibody was captured from the culture supernatant by protein A chromatography followed by a hydrophobic interaction purification step involving phenyl -sepharose chromatography. Additional glycoforms were generated by post-purification enzymatic treatment with α-1,2 mannosidase, β-N-acetylglucosaminidase and β-1,4 galactosyltransferase. After purification, the antibodies were characterized by nonreducing SDS-PAGE to assess proper assembly. Antibodies derived from *P. pastoris* showed similar migration behavior to controls from cultured Chinese hamster ovary cells (**Fig. 1a**). Antigen affinity was determined by a cell-based binding assay using Wil2-S cells, which overexpress CD20 on their cell surface. As expected, glycosylation variants did not show different antigen-binding characteristics. A representative binding curve is shown for GS4.0 (**Fig. 1b**). Glycans were analyzed by matrix-assisted laser desorption ionization/time-of-flight (MALDI-TOF) mass spectrometry after release from the antibody with peptide-*N*-glycosidase F[9] (**Fig. 2**). Seven different glycoforms of rituximab were generated and compared to commercial rituximab. Of these seven glycoforms, two were of the complex human type (GS 4.0 and GS 5.0) that typically represent a minor fraction (<5%) of all glycans present in antibodies produced by Chinese hamster ovary cells (**Fig. 2a**)[5]. The other glycovariants were

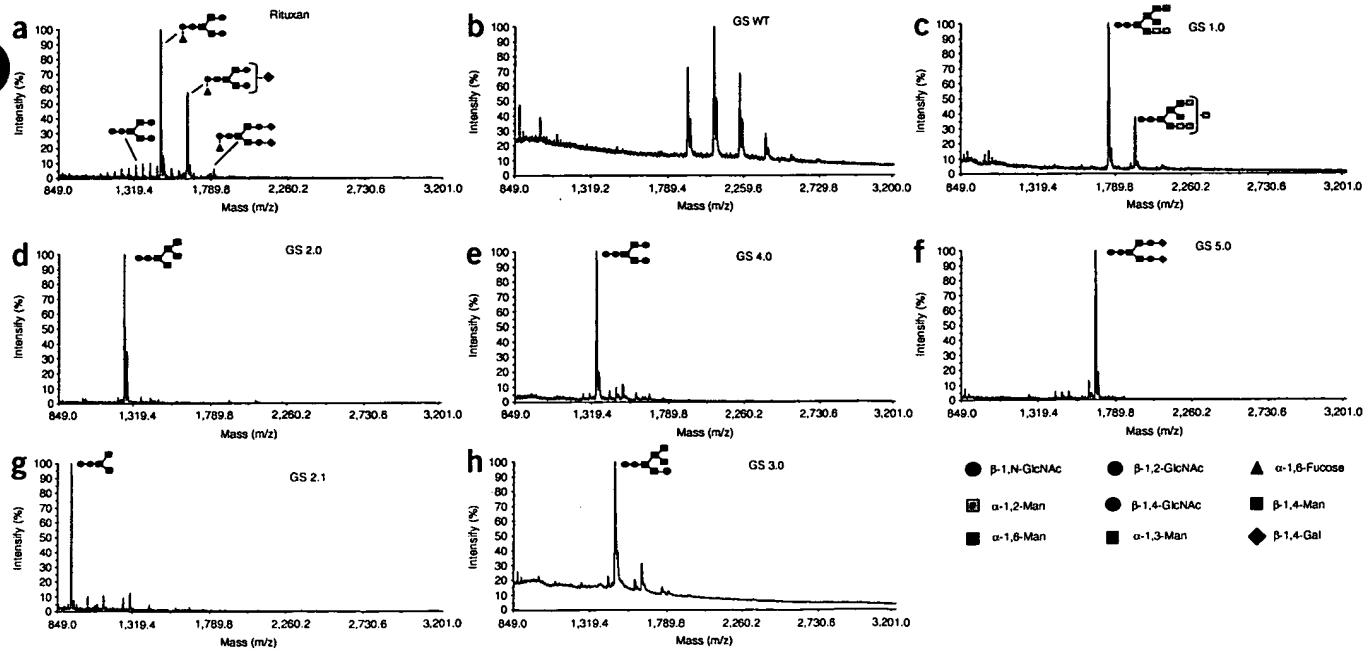

Figure 2 N-glycan analysis of antibodies. MALDI-TOF mass spectrometry of oligosaccharides released from rituximab. (**a–h**) Rituxan (**a**), *P. pastoris* wild-type (WT) (**b**) and glycoengineered strains of *P. pastoris* (**c–h**).

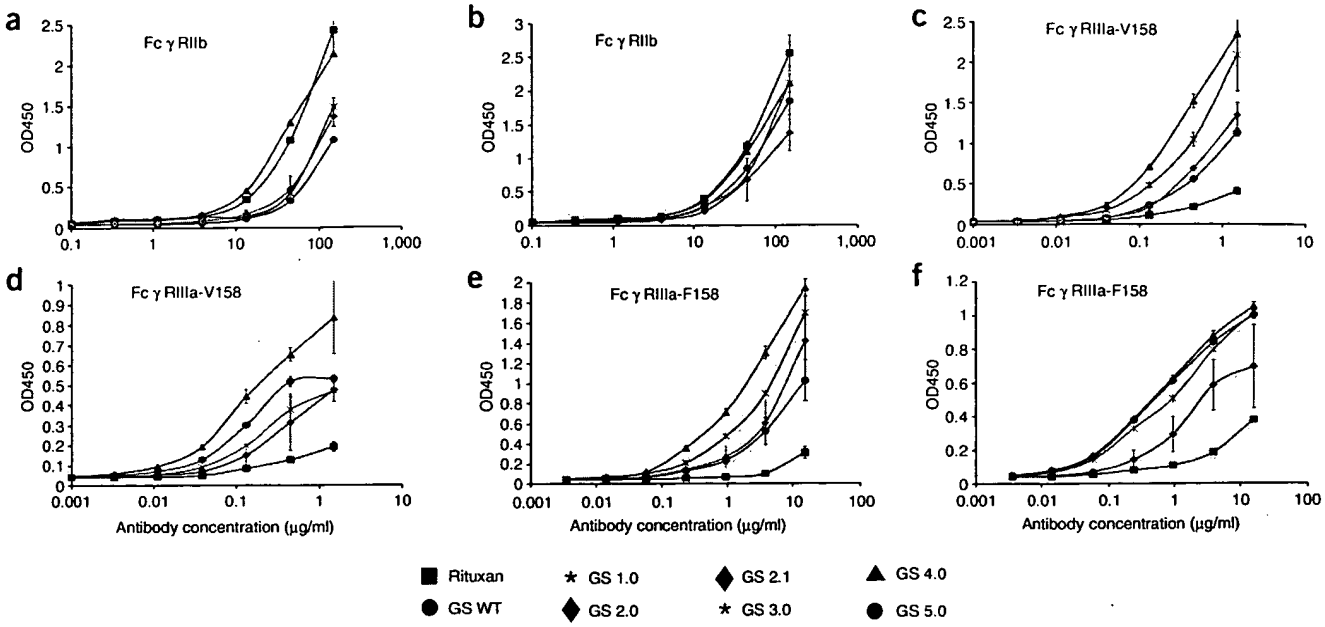

Figure 3 Receptor binding assays of rituximab glycovariants. (**a–f**) Binding to human FcγRIIb (**a,b**), FcγRIIIa 158V (**c,d**), FcγRIIIa 158F (**e,f**).

of the high mannose type, including wild-type *P. pastoris* glycans (mostly Man9–Man12 with α-1,6 mannose extensions to the core, designated GS WT), the human intermediates Man5 (GS 2.0) and Man8 (GS 1.0) that are common byproducts found in mammalian cell culture, a trimannose core structure (GS 2.1), as well as a hybrid structure (GS 3.0). Receptor-binding assays focused on the stimulatory receptor FcγRIIIa-V158, its low affinity polymorphic form FcγRIIIa-F158 and the inhibitory receptor FcγRIIb (**Fig. 3**), although other Fcγ receptors were also tested (data not shown). Fcγ receptor-binding assays showed that changing the glycan structures of the antibody improved binding affinities for FcγRIIIa-V158 at least tenfold compared to commerical rituximab. The binding affinities (in decreasing order) were: GS 4.0 > GS 5.0 > GS 3.0 > > > Rituxan (**Fig. 3c,d**). Binding to the low-affinity variant FcγRIIIa-F158 can be improved over 100-fold with binding affinities decreasing in the order GS 4.0, GS 5.0 > GS 3.0 > > > Rituxan (**Fig. 3e,f**).

Finally, three specific glycoforms were compared with commercial rituximab in a B-cell depletion assay (**Fig. 4**). This assay measures antibody-mediated killing and was able to demonstrate both improved B-cell depletion for glycoengineered variants compared with the mammalian cell culture–derived product, as well as improved B-cell depletion in a blood matrix assay for glycoengineered IgGs with elevated FcγRIIIa and lower FcγRIIb binding affinities. Glycosylation by wild-type *P. pastoris* results in no measurable B-cell depletion, whereas specific glycoforms obtained from glycoengineered yeast strains showed a more efficient depletion of CD19 positive B-cells than the mammalian cell–derived mixture of glycoforms present in the commercial product (**Fig. 4**). It is worth noting that the receptor-binding affinity and B-cell depletion potency for commercial rituximab is the collective action of many different glycoforms of varying potencies (**Figs. 2** and **4**). It is also surprising that wild-type *P. pastoris* glycoforms were able to mediate stronger binding to FcγRIIIa while at the same time showing lower affinity to FcγIIb when compared to commercial rituximab. Nevertheless, these wild-type glycoforms displayed virtually no B-cell depletion in a blood matrix assay. This may result from the presence of macrophage mannose receptors that bind to high mannose glycans and interfere with the antibody's interaction with Fcγ receptors.

These experiments show that controlling glycan composition and structure on IgGs may be an important approach for improving the therapeutic efficacy of mAbs. Moreover, general protein optimization and engineering efforts, which have focused primarily on the polypeptide sequence, can now be expanded to include optimization of the glycan composition of glycoproteins. In the past, this was restricted by the choice of expression host and was either limited to the natural repertoire of glycoforms produced by a given host or involved extensive purification efforts to enrich particular glycoforms. Although the present work focuses on optimizing antibody binding to two Fcγ receptors, other glycosylation-dependent properties such as

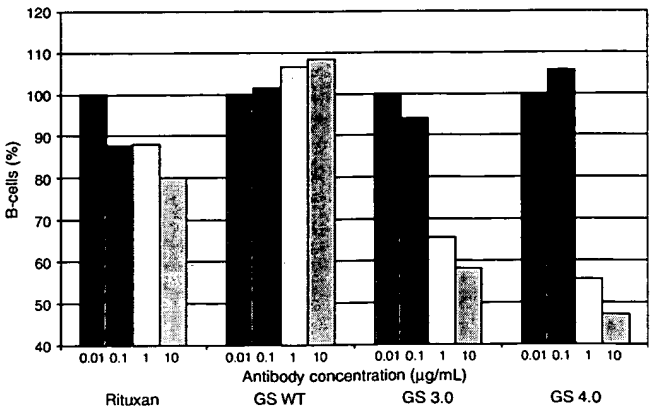

Figure 4 B-cell depletion assays of rituximab/Rituxan, GS WT, GS3.0 and GS4.0. 100% corresponds to a ratio of CD19-positive B cells to total CD45-positive leucocytes of 0.11.

solubility, *in vivo* half-life, tissue distribution[13] and interaction with complement proteins[14] can likely be improved by using libraries of glycoforms generated by glycoengineered yeast strains. Ongoing efforts to expand the library of glycoengineered yeast cell lines are expected to yield a large array of specific glycovariants that were hitherto unobtainable on a commercial scale using cultured mammalian cells. As scaled-up production of recombinant proteins in yeast is a mature and well-established technology, it seems reasonable to contemplate the high-throughput and cost-effective production of particular designer glycoforms using glycoengineered yeast strains.

METHODS

Strains and reagents. *Escherichia coli* strains TOP10 or DH5α were used for recombinant DNA work. Restriction endonucleases, DNA modification enzymes and *N*-glycosidase F were obtained from New England BioLabs. Oligonucleotides were obtained from Integrated DNA Technologies. Salts and buffers were obtained from Sigma and MALDI matrices were obtained from Aldrich.

Yeast strains for mAb expression and Fc receptors. Plasmid pDX 478 (**Supplementary Fig. 1** online), which contains anti-CD20 heavy and light chain with a Kar2 signal peptide, was expressed in a wild-type strain of *P. pastoris* NRRL Y-11430 yielding typical *Pichia* glycans of the high mannose type (GS WT, **Fig. 2b**), and several glycoengineered cell lines including YGLY14 [Δoch1, Δbmt2, Δmnn4B, Δpno1, SUC2] yielding glycans (GS1.0) (**Fig. 2c**), and YAS309 [Δoch1, Δpno1, Δmnn4B, Δbmt2, *Kluyveromyces lactis* UDP-GlcNAc transporter, α-1,2 *Mus musculus* MnsI, β-1,2 GlcNAc transferase I, β-1,2 *Rattus norvegicus* GlcNAc transferase II, *Drosophila melanogaster* MnsII, *Schizosaccharomyces pombe* Gal epimerase, *D. melanogaster* UDP-Gal transporter, *Homo sapiens* β-1,4 galactosyl transferase] yielding glycans GS 4.0 after *in vitro* galactosidase treatment (**Fig. 2e**). All strains were constructed according to the methods described earlier[9,10]. Plasmid pDX 482, which contains CD-20 heavy and light chain with a chicken lysozyme signal sequence, was expressed in YAS385-1 [Δoch1, Δpno1, Δmnn4B, Δbmt2, *K.lactis* UDP-GlcNAc transporter, α-1,2 *M. musculus* MnsI, β-1,2 GlcNAc transferase I, β-1,2 *Rattus norvegicus* GlcNAc transferase II, *D. melanogaster* UDP-Gal transporter, *H. sapiens* β-1,4 galactosyl transferase] to yield glycan structures GS3.0 after *in vitro* galactosidase treatment (**Fig. 2h**).

Fcγ receptors were expressed in YAS309 resulting in GS5.0 glycosylation (see below).

DNA sequence of *P. pastoris* Kar2 signal peptide. GAATTCGAAACGATGCTGTCGTTAAAACCATCTTGGCTGACTTTGGCGGCATTAATGTATGCCATGCTATTGGTCGTAGTGCCATTTGCTAAACCTGTTAGAGCT. Underlined is *Eco*R1 site and Kozak sequence. DNA sequence of chicken lysozyme signal sequence. GAATTCGAAACGATGCTGGGTAAGAACGACCCAATGTGTCTTGTTTTGGTCTTGTTGGGATTGACTGCTTTGTTGGGTATCTGTCAAGGT. Underlined is *Eco*R1 site and Kozak sequence.

Construction of antibody expression vectors. Sequence of anti-CD20 was based on US patent 6,682,734 (ref. 15). There are multiple patents covering rituximab sequences in the patent literature with a total of two amino acid variations at amino acid position 14 of the heavy chain (proline/valine). The sequence used in this study conforms with the sequence published in US patent 6,682,734 with a proline at position 14 in the variable region of the heavy chain and a G1m(z,a) allotype in the constant region of the heavy chain. This sequence was chosen based on liquid chromatography–mass spectrometry peptide mapping that allowed us to exclude valine at position 14 of the heavy chain and is listed below:

Heavy chain.

(1) QVQLQQPGAE LVKPGASVKM SCKASGYTFT SYNMHWVKQT PGRGLEWIGA (51) IYPGNGDTSY NQKFKGKATL TADKSSSTAY MQLSSLTSED SAVYYCARST (101) YYGGDWYFNV WGAGTTVTVS AASTKGPSVF PLAPSSKSTS GGTAALGCLV (151) KDYFPEPVTV SWNSGALTSG VHTFPAVLQS SGLYSLSSVV TVPSSSLGTQ (201) TYICNVNHKP SNTKVDKKAE PKSCDKTHTC PPCPAPELLG GPSVFLFPPK (251) PKDTLMISRT PEVTCVVVDV SHEDPEVKFN WYVDGVEVHN AKTKPREEQY (301) NSTYRVVSVL TVLHQDWLNG KEYKCKVSNK ALPAPIEKTI SKAKGQPREP (351) QVYTLPPSRD ELTKNQVSLT CLVKGFYPSD IAVEWESNGQ PENNYKTTPP (401) VLDSDGSFFL YSKLTVDKSR WQQGNVFSCS VMHEALHNHY TQKSLSLSPG (451) K

The light chain was of the Km3 allotype and is listed below:

Light chain.

(1) QIVLSQSPAI LSASPGEKVT MTCRASSSVS YIHWFQQKPG SSPKPWIYAT (51) SNLASGVPVR FSGSGSGTSY SLTISRVEAE DAATYYCQQW TSNPPTFGGG (101) TKLEIKRTVA APSVFIFPPS DEQLKSGTAS VVCLLNNFYP REAKVQWKVD (151) NALQSGNSQE SVTEQDSKDS TYSLSSTLTL SKADYEKHKV YACEVTHQGL (201) SSPVTKSFNR GEC.

Constant regions of heavy chain and light chain were obtained from GeneArt. Anti-CD20 L and anti-CD20 H were synthesized by PCR using overlapping oligonucleotides. PCR products were cloned into pCR2.1Topo vector (Invitrogen) to form pDX343 and pDX360. The *NotI* and *MlyI* fragments of heavy chain and light chain were cut from pDX360 and pDX343, and cloned downstream of a Kar2 signal sequence into pPICZa (Invitrogen) to form pDX468 and pDX344. Heavy chain and Light chain were combined by overlap PCR and cloned into the single vector pBK85 using the primers listed below to generate pDX478. Construction of pDX482 is identical to pDX478 except the signal sequence is chicken lysozyme instead of Kar2 signal sequence (see **Supplementary Fig. 1** online).

HchainASTKGPS/up; GCTTCTACTAAGGGACCATCC
HchainASTKGPS/lp; GGATGGTCCCTTAGTAGAAGC
CD20H/up; AGGAGTCGTATTCAAGTCCAG
HFckpn1/lp; CTGGTAttaCTTACCTGGGGACAAAGAC
CD20L/up; AGgagtcgtattCAAATCGTC
LfusionRTVAAPS/up; AGAACTGTTGCTGCTCCATCC
LfusionRTVAAPS/lp; GGATGGAGCAGCAACAGTTC
CD20L/lp; ctggtaccttaACACTCTCCTCTGTTGAAG

Genealogy of plasmids. pDX343 (anti-CD20L chain in pCR2.1 topo vector)
pDX360 (anti-CD20H chain in pCR2.1 topo vector)
pDX344 (anti-CD20L chain in pPICZa vector)
pDX468 (anti-CD20H chain in pPICZa vector)
pDX478 (anti-CD20H and anti-CD20L in the single vector pBK85)

Cloning of soluble FcγRIIIa domains. Soluble human FcγRIIIa F158 (Ala16-Gln208) (accession no. NP000560), with a Gly_3His_9 C-terminal tail was codon optimized for expression in *P. pastoris* and synthesized by GeneArt to form pAS198. The chimeric gene was cloned into pPICZa (Invitrogen) as an *AfeI*/*KpnI* fragment with a *Sc*MFprepro signal sequence *Eco*RI/blunt fragment. The resulting plasmid was sequence verified and named pAS252. The FcγRIIIa-V158 polymorphism was created by site-directed mutagenesis. PCR amplification of FcγRIIIA from pAS198 was performed using TaqUltra *Pfu*, forward primer TAS505 (5′-AGAGGATTGGTTGGTTCCAAGAACGTTTCTTCC-3′), reverse primer TAS506 (5′-CTTGGAACCAACCAATCCTCTACAGAAGTAG GA-3′), *Pfu* reaction buffer and dNTPS. The PCR product was digested with *DpnI* and transformed into XL10 Gold *E. coli* (Stratagene). The presence of the FcγRIIIA V158 mutation was confirmed by DNA sequencing and the resulting plasmid construct was named pAS226. The FcγRIIIA V158 gene was cloned into pPICZα as an *AfeI*/*KpnI* fragment with a *Sc*MFprepro signal sequence *Eco*RI/blunt fragment to form pAS271.

Recombinant expression of FcγRIIIa receptors. YAS309 was used as the host strain for expression of FcγRIIIa. Briefly, yeast cells was harvested in the logarithmic phase by centrifugation and washed three times with ice-cold 1 M sorbitol. Ten micrograms of *PmeI*-digested pAS252 or pAS271 was mixed with competent yeast cells and electroporated using a BTX Electro Cell Manipulator. After electroporation, cells were suspended in 1 ml of 1 M sorbitol and allowed to recover for 1 h at 25 °C. Cells were then spread onto YPD plates containing 100 μg/ml Zeocin and incubated at 25 °C. Twenty-four transformants were inoculated in buffered glycerol-complex medium (BMGY) medium and grown for 72 h followed by a 24 h induction in buffered methanol-complex medium (BMMY) medium. Secretion of FcγRIIIa receptor was assessed by dot blot immunoassay using mouse anti-human FcγRIIIa. High expressing clones were further characterized by nickel-affinity purification followed by MALDI-TOF analysis (data not shown).

Fermentation conditions. The primary culture was prepared by inoculating a 1-L baffled flask containing 200 ml of BMGY media with 10 ml of a seed culture. The cells from the primary culture were transferred to inoculate the fermenter. The fermentation medium contained: 40 g glycerol; 15 g sorbitol; 2.3 g K_2HPO_4; 11.9 g KH_2PO_4; 10 g yeast extract; 20 g peptone; 1 g casein amino acids; 4×10^{-3} g biotin; 13.4 g YNB; per liter of medium.

Fermentations were conducted in 3 L (1.5 L initial volume) dished-bottom Applikon bioreactors. The fermenters were run in fed-batch mode under the following conditions: the temperature was set at 24 °C and the pH was adjusted to 6.5 with NH_4OH. The dissolved oxygen (DO) was maintained at 20% by adjusting agitation rate (450–1,000 r.p.m.) and addition of pure oxygen. The airflow rate was maintained at 0.5 vvm. After depletion of the initial glycerol (40 g/L) a 50% glycerol solution containing 12 ml/L PTM1 salts[11] was fed at an average rate of 8 ml/L/h until the desired biomass of 250 g $_{WCW}$/L was reached. After a 30 min starvation period the methanol feed (100% methanol with 12 ml/L PTM1 salts) was initiated. An exponential feeding rate beginning with 3 g/L/h and increasing at a specific rate of 0.01 1/h was continued for 30 to 40 h. After the fermentation the supernatant was obtained by centrifugation and used for further purification of the antibody.

Antibody purification. The antibody was captured by affinity chromatography from the supernatant medium of *P. pastoris* fermentations using a Streamline rProtein A resin from GE Healthcare. The resin was equilibrated with 50 mM Tris-HCl pH 7 and the supernatant medium was adjusted at the same pH. The column was washed with 4 column volumes of the same buffer and the antibody was eluted with 100 mM Glycine-HCl pH 3. The eluted protein was neutralized immediately with 1 M Tris-HCl, pH 7.

A phenyl sepharose fast flow resin (GE Healthcare) was used as a second purification step. The column was equilibrated in 20 mM Tris-HCl pH 7, 1 M $(NH_4)_2SO_4$ and the sample obtained from the first column was applied to the phenyl sepharose column after adding $(NH_4)_2SO_4$ to a final concentration of 1 M. The elution was performed by developing a gradient over 10 column volumes ranging from 1 M to 0 M $(NH_4)_2SO_4$ in 20 mM Tris-HCl, pH 7. The antibody elutes around 500–400 mM $(NH_4)_2SO_4$. The pooled protein was dialyzed against PBS and stored a –80 °C.

Fcγ receptor purification. Fcγ receptors were purified by two chromatographic steps. The first column was a Streamline Chelating resin (GE Healthcare) charged with nickel and equilibrated with 20 mM Tris-HCl pH 7.9, 200 mM NaCl. The supernatant medium was adjusted to the same pH and then applied directly to the column. The column was washed with 5 column volumes using the same buffer and the protein was eluted with an imidazol gradient (0–0.5 M) developed over 10 column volumes. The Fcγ receptor elutes around 200 mM imidazol. The pool obtained from the chelating column was adjusted with $(NH_4)_2SO_4$ to a final concentration to 1.5 M, and loaded onto a phenyl sepharose fast flow column (equilibrated with 20 mM Tris-HCl pH 7, 1.5 M $(NH_4)_2SO_4$). Elution of the protein was performed with a gradient ranging from 1.5 to 0 M $(NH_4)_2SO_4$ (over 10 column volumes). The purified protein fraction was dialyzed against PBS and stored at −80 °C for future use in enzyme-linked immosorbent assay–based receptor-binding assays.

***In vitro* galactose transfer.** YAS 309 does not transfer galactose efficiently on antibodies because of the steric hindrance of the glycan positioned at Asn 297 of the heavy chain. To obtain more homogenous glycoforms, we performed *in vitro* galactosidase digest and galactose transfer to obtain uniform GS 4.0 and GS 5.0 respectively. Purified antibody (GS 4.0) was buffer exchanged to 50 mM MES (pH 6.4), by passing through an Amicon Ultra-15 10,000 Molecular Weight Cut Off at 2,500 r.p.m. at 600*g*. The protein was then incubated with β-1,4-galactosyltransferase (GalT, Bovine, recombinant, EMD Biosciences) and UDP-Galactose (UDP-Gal, 25 mg/ml, Sigma) in 50 mM MES (pH 6.4), 5 mM $MnCl_2$ at 24 °C O/N to yield glycan structures GS5.0 (see **Fig. 2f**). Protein and UDP-Gal and GalT ratio for antibody: 10 mg:625 μg:500 mU GalT. Antibody was purified using a SP-sepharose (GE Healthcare) fast-flow resin with 0–1 M NaCl in 50 mM sodium acetate, pH 5.2.

***In vitro* enzymatic digest.** β1-4-galactosidase, β1-2,3,4,6-N-acetylglucosaminidase (EMD Biosciences) was used to generate GS2.1 from GS4.0, and α1,2 mannosidase (a gift from Roland Contreras, Unit of Fundamental and Applied Molecular Biology, Department of Molecular Biology, Ghent University, Ghent, Belgium) was used to generate GS2.0 from GS1.0. Digests were performed in 50 mM ammonium acetate pH 5.0 at 37 °C overnight. Antibody was purified using a SP-sepharose (GE Healthcare) fast flow resin with 0-1 M NaCl in 50 mM sodium acetate pH 5.2.

MALDI-TOF analysis of glycans. N-glycans were released and separated from the glycoprotein as described earlier[9,10]. Molecular weight was determined by using a Voyager PRO linear MALDI-TOF (Applied Biosystems) mass spectrometer with delayed extraction[9,10].

Antigen-binding assay. The antigen-binding assay was carried out using human B-lymphoblastoid WIL2-S cells (American Type Culture Collection) according to methods described[16]. In brief, 200 μl of a Wil2-S cell suspension (1.5×10^6 Wil2-S cells/200 μl of assay buffer) was added to each well of a 96-well round-bottom plate (Nunc) and centrifuged at 4 °C at 500*g*. Supernatants were removed by aspiration and antibody solutions were added (100 μl per well) in concentrations ranging from 2 μg/ml to 2.74 ng/ml, including an assay buffer-only control; plates were agitated to suspend cells. Plates were incubated on ice for 45 min, centrifuged and washed three times with assay buffer (3 × 200 μl/well). After the final wash, 100 μl of 1:2,000 anti-Fc horseradish peroxidase (HRP) conjugate (Sigma) were added to each well, and incubated on ice. Plates were washed as above and developed with 100 μl TMB (Sigma) at 24 °C. Reaction was stopped by the addition of 1 M H_2SO_4. Plates were centrifuged and supernatants were transferred to a 96-well flat bottom plate (Corning Costar) and the absorbance at 450 nm was determined in a 96-well plate reader (Tecan, Genios Plus). An antibody against human HER2 was used as a negative control.

Fcγ receptor binding assay. Fcγ receptor–binding assays were carried out as described[17] with minor modifications. High-protein-binding 96-well plates (Corning Costar) were coated with 100 μl per well of Fcγ receptor solutions in PBS, 1% BSA at the following concentrations: 2 μg/ml for Fcγ IIb (R&D systems), 0.4 μg/ml for Fcγ IIIa-V158 (see above) and 0.8 μg/ml Fcγ IIIa-F158 (see above). The bound antibody was detected using HRP-conjugated goat-$F(ab')_2$ anti-human $F(ab')_2$ (Jackson Immunoresearch) and quantified by measuring the OD_{450}.

B-cell depletion assay. B-cell depletion assay was performed as described[18]. In brief, heparinized blood samples were collected from healthy volunteers, from whom informed consent was obtained, at the Dartmouth Hitchcock Medical Center, Lebanon, New Hampshire, and the homozygous FcγRIIIa-F158 genotype was confirmed by PCR amplification followed by restriction endonuclease digest (data not shown). Blood samples was spun for 5 min at 1,800 r.p.m. at 600*g*, the supernatant (plasma) was discarded, and the pellet was treated with the ACL reagent (Ammonium Chloride Lysing reagent: 0.15 M NH_4Cl, 10 mM $NaHCO_3$, 80 μM tetrasodium EDTA, pH 7.4), washed and resuspended in an equivalent volume of stain buffer. Leucocytes suspended in 90 μl of stain buffer were incubated with 10 μl of rituximab (concentrations from 0.1–100 μg/ml) or stain buffer for 60 min at 37 °C. Samples were stained immediately with anti-CD19 plus fluorescein isothiocyanate (FITC) and anti-CD45 plus phycoerythrin (PE) and analyzed by flow cytometry (FACScan, Becton Dickinson). In the negative control (no addition of rituximab antibody) the ratio was about 0.11 (data not shown), which was used as the baseline for the total B-cell population (that is, 100% in **Fig. 4**).

Note: Supplementary information is available on the Nature Biotechnology website.

ACKNOWLEDGMENTS

We wish to acknowledge Ron Hitzman and Max Vasquez for their continued input on improving antibody expression and quality. Erin Giaccone, Sujatha Gomathinayagam, Heather Lynaugh, Teresa Mitchell and Alissa Thompson are acknowledged for excellent technical assistance and Jim Posada is acknowledged for his insistence on developing a yeast-based antibody expression platform.

COMPETING INTERESTS STATEMENT

The authors declare competing financial interests (see the *Nature Biotechnology* website for details).

Published online at http://www.nature.com/naturebiotechnology/
Reprints and permissions information is available online at http://npg.nature.com/reprintsandpermissions/

1. Weiner, L.M. & Carter, P. Tunable antibodies. *Nat. Biotechnol.* **23**, 556–557 (2005).
2. Rothman, R.J., Perussia, B., Herlyn, D. & Warren, L. Antibody-dependent cytotoxicity mediated by natural killer cells is enhanced by castanospermine-induced alterations of IgG glycosylation. *Mol. Immunol.* **26**, 1113–1123 (1989).
3. Lifely, M.R., Hale, C., Boyce, S., Keen, M.J. & Phillips, J. Glycosylation and biological activity of CAMPATH-1H expressed in different cell lines and grown under different culture conditions. *Glycobiology* **5**, 813–822 (1995).
4. Umaña, P. *et al.* Engineered glycoforms of an antineuroblastoma IgG1 with optimized antibody-dependent cellular cytotoxic activity. *Nat. Biotechnol.* **17**, 176–180 (1999).
5. Shields, R.L. *et al.* Lack of fucose on human IgG1 *N*-linked oligosaccharide improves binding to human FcγRIII and antibody-dependent cellular toxicity. *J. Biol. Chem.* **277**, 26733–26740 (2002).
6. Shinkawa, T. *et al.* The absence of fucose but not the presence of galactose or bisecting *N*-acetylglucosamine of human IgG1 complex-type oligosaccharides shows the critical role of enhancing antibody-dependent cellular cytoxicity. *J. Biol. Chem.* **278**, 3466–3473 (2003).
7. Clynes, R.A., Towers, T.L., Presta, L.G. & Ravetch, J.V. Inhibitory Fc receptors modulate *in vivo* cytoxicity against tumor targets. *Nat. Med.* **6**, 443–446 (2000).
8. Cartron, G. *et al.* Therapeutic activity of humanized anti-CD20 monoclonal antibody and polymorphism in IgG Fc receptor FcγRIIIa gene. *Blood* **99**, 754–758 (2002).
9. Choi, B.-K. *et al.* Use of combinatorial genetic libraries to humanized N-linked glycosylation in the yeast *Pichia pastoris*. *Proc. Natl. Acad. Sci. USA* **100**, 5022–5027 (2003).
10. Hamilton, S. *et al.* Production of complex human glycoproteins in yeast. *Science* **301**, 1244–1246 (2003).
11. Bobrowicz, P. *et al.* Engineering of an artificial glycosylation pathway blocked in core oligosaccharide assembly in the yeast *Pichia pastoris*: Production of complex humanized glycoproteins with terminal galactose. *Glycobiology* **14**, 757–766 (2004).
12. Gerngross, T.U. Advances in the production of human therapeutic proteins in yeasts and filamentous fungi. *Nat. Biotechnol.* **22**, 1409–1414 (2004).
13. Wright, A. *et al. In vivo* trafficking and catabolism of IgG1 with Fc associated carbohydrates of differing structure. *Glycobiology* **10**, 1347–1355 (2000).
14. Wright, A. & Morrison, S.L. Effect of C2-associated carbohydrate structure on Ig effector function: studies with chimeric mouse-human IgG1 antibodies in glycosylation mutants of Chinese hamster ovary cells. *J. Immunol.* **160**, 3393–3402 (1998).
15. Anderson, D.R. *et al.* Therapeutic application of chimeric and radiolabeled antibodies to human B lymphocyte restricted differentiation antigen for treatment of B cell lymphoma. US Patent No. 6,682,734 (1995).
16. Hong, K. *et al.* Simple quantitative live cell and anti-idiotypic antibody based ELISA for humanized antibody directed to cell surface protein CD20. *J. Immunol. Methods* **294**, 189–197 (2004).
17. Shields, R.L. *et al.* High resolution mapping of the binding site on human IgG1 for FcγRI, FcγRII, FcγRIII and FcRn and design of IgG1 variants with improved binding to the FcgR. *J. Biol. Chem.* **276**, 6591–6604 (2001).
18. Vugmeyster, Y. & Howell, K. Rituximab-mediated depletion of cynomolgus monkey B cells *in vitro* in different matrices: possible inhibitory effect of IgG. *Int. Immunopharmacol.* **4**, 1117–1124 (2004).